Molecular Vision 2013; 19:2615-2625 <http://www.molvis.org/molvis/v19/2615>
Received 17 July 2013 | Accepted 27 December 2013 | Published 31 December 2013

Presence of the *Gpr179*^{nob5} allele in a C3H-derived transgenic mouse

Jasmin Balmer,[1,2] Rui Ji,[3] Thomas A. Ray,[3] Fabia Selber,[1] Max Gassmann,[4] Neal S. Peachey,[5,6,7] Ronald G. Gregg,[3] Volker Enzmann[1]

[1]Department of Ophthalmology, Inselspital, University of Bern, Switzerland; [2]Graduate School for Cellular and Biomedical Sciences, University of Bern, Switzerland; [3]Department of Biochemistry and Molecular Biology, University of Louisville, KY; [4]Institute of Veterinary Physiology, University of Zürich, Switzerland; [5]Department of Ophthalmic Research, Cole Eye Institute, Cleveland Clinic, Cleveland OH; [6]Research Service, Louis Stokes Cleveland VA Medical Center, Cleveland OH; [7]Department of Ophthalmology, Cleveland Clinic Lerner College of Medicine of Case Western Reserve University, Cleveland OH

Purpose: To identify the mutation responsible for an abnormal electroretinogram (ERG) in a transgenic mouse line (tg21) overexpressing erythropoietin (Epo). The tg21 line was generated on a mixed (C3H; C57BL/6) background and lacked the b-wave component of the ERG. This no-b-wave (nob) ERG is seen in other mouse models with depolarizing bipolar cell (DBC) dysfunction and in patients with the complete form of congenital stationary night blindness (cCSNB). We determined the basis for the nob ERG phenotype and screened C3H mice for the mutation to evaluate whether this finding is important for the vision research community.

Methods: ERGs were used to examine retinal function. The retinal structure of the transgenic mice was investigated using histology and immunohistochemistry. Inverse PCR was performed to identify the insertion site of the Epo transgene in the mouse genome. Affected mice were backcrossed to follow the inheritance pattern of the nob ERG phenotype. Quantitative real-time PCR (qRT PCR), Sanger sequencing, and immunohistochemistry were used to identify the mutation causing the defect. Additional C3H sublines were screened for the detected mutation.

Results: Retinal histology and blood vessel structure were not disturbed, and no loss of DBCs was observed in the tg21 nob mice. The mutation causing the nob ERG phenotype is inherited independently of the tg21 transgene. The qRT PCR experiments revealed that the nob ERG phenotype reflected a mutation in *Gpr179*, a gene involved in DBC signal transduction. PCR analysis confirmed the presence of the *Gpr179*^{nob5} insertional mutation in intron 1 of *Gpr179*. Screening for mutations in other C3H-derived lines revealed that C3H.Pde6b^{+} mice carry the *Gpr179*^{nob5} allele whereas C3H/HeH mice do not.

Conclusions: We identified the presence of the *Gpr179*^{nob5} mutation causing DBC dysfunction in a C3H-derived transgenic mouse line. The nob phenotype is not related to the presence of the transgene. The *Gpr179*^{nob5} allele can be added to the list of background alleles that impact retinal function in commonly used mouse lines. By providing primers to distinguish between *Gpr179* mutant and wild-type alleles, this study allows investigators to monitor for the presence of the *Gpr179*^{nob5} mutation in other mouse lines derived from C3H.

The purpose of this report is to define the underlying cause of an electroretinogram (ERG) abnormality noted in a transgenic mouse line (tg21) designed to overexpress erythropoietin (Epo) in the retina and the brain. The original goal of the study was to evaluate the potential of Epo for neuroprotection since Epo is beneficial in several animal models [1-3]. ERG analysis of multiple tg21 animals noted that the ERG a-wave, reflecting activity of retina photoreceptors [4], was retained while the b-wave, representing the response of depolarizing bipolar cells (DBCs) [5], was absent. This no-b-wave (nob) phenotype was similar to that reported for mouse models of DBC dysfunction due to mutations in Nyctalopin (*Nyx*) [6], G-protein coupled receptor 179 (*Gpr179*) [7], Glutamate receptor metabotropic 6 (*Grm6*) [8], or Transient receptor potential cation channel subfamily M member 1 (*Trpm1*) [9-12].

To understand the basis of the nob ERG phenotype of tg21 mice, we conducted a series of morphological and molecular studies to evaluate potential explanations. We also performed a mapping cross to identify the locus of the gene involved. These studies demonstrated that the nob ERG phenotype was not associated with a loss of retinal neurons including DBCs, or abnormal retinal vasculature. In fact, the ERG nob phenotype was inherited independently of the tg21 transgene. We measured gene expression levels for *Nyx*, *Gpr179*, *Grm6*, and *Trpm1* and found that *Gpr179* was significantly decreased in affected animals. Further analysis indicated that the nob ERG phenotype reflected a large insertion in the *Gpr179* locus, the

Correspondence to: Volker Enzmann, Department of Ophthalmology, Freiburgstrasse 14, 3010 Bern, Switzerland, Phone: 0041/ 31632-8935; FAX: 0041/31632-4882; email: Volker.Enzmann@insel.ch

same mutation recently reported in *Gpr179*^{nob5} mice [7], and that this mutation is present in additional C3H-derived mouse lines. We provide evidence that mice investigated by Hoelter and colleagues characterized by a nob ERG phenotype carry the *Gpr179*^{nob5} mutation [13]. These observations indicate that the *Gpr179*^{nob5} mutation likely appeared many years ago, and that it may be present in additional lines beyond those examined here.

METHODS

Mice: The tg21 mice were originally generated to study the effect of constitutively overexpressed Epo in vascular diseases [14] and were provided by Prof. Max Gassmann, University of Zürich. They were bred to create a line homozygous for the transgene and were maintained in a 12 h:12 h light-dark cycle with food and water ad libitum. To map the trait underlying the nob ERG phenotype, affected tg21 mice were mated to DBA/2N mice (Charles River WIGA, Sulzfeld, Germany) to generate F1 progeny. F1 mice were intercrossed to generate the F2 progeny used for mapping based on ERG analysis. C57BL/6 mice were obtained from Charles River. Experiments were conducted according to the Association for Research in Vision and Ophthalmology (ARVO) Statement for the Use of Animals in Ophthalmic and Vision Research following government approval.

We also examined genomic DNA from C3H/HeH and C3H.Pde6b^{+} mice generously provided by Dr. Martin Fray (MRC Harwell, Oxfordshire, UK) and from C57BL/6 and *Gpr179*^{nob5} mice.

Molecular cloning of the erythropoietin insertion site in tg21: Genomic DNA was isolated using the Gen Elute Mammalian Genomic DNA Miniprep Kit (Sigma Aldrich, St. Louis, MO). Inverse PCR was used to clone sequences flanking the Epo transgene. Briefly, primers were designed to the known sequence adjacent to an EcoRI restriction site located in the known platelet-derived growth factor (PDGF) promoter. Following enzymatic digestion using EcoRI, the enzyme was inactivated by heating at 65 °C for 15 min, the DNA was diluted, and T4 DNA ligase added to circularize the EcoRI fragments. This DNA was used as input for PCR using AccuPrime Taq Polymerase (Invitrogen Life Technologies, Carlsbad, CA) and the primer pair tg21 inv1 and tg21 inv2 (Table 1) as recommended by the manufacturer. A 600 bp junction fragment was amplified and sequenced to identify the genomic insertion site of the tg21 Epo transgene.

For genotyping purposes, genomic DNA was isolated as described, and F2 animals were genotyped for the Epo insertion and for markers specific to the wild-type flanking sites of the Epo insertion site. Primers used are listed in Table 1. The Epo insert was identified with PCR using the primers 5′-hPDGF of the human promoter and the 3′-hPDGF primer [15]. To differentiate between tg21/tg21 homozygous and tg21/+ heterozygous animals, a PCR using primers on chromosome 8 (Primer Chr8–01, Chr8–03) that flank the transgene was used. PCR amplifications were performed using the iQ SYBR Green Supermix (BioRad, Cressier, Switzerland) on a MyiQ single color Real-time PCR detection system (BioRad). Cycling conditions were 45 cycles comprising a 30 s step of denaturation at 95 °C, a 30 s annealing step at 60 °C (for Chr8–01/Chr8–03 primers) or 64 °C (for hPDGF primers), and a 30 s extension period at 72 °C.

Electroretinography: Animals were dark-adapted overnight, and all procedures were performed under dim red light. Mice were anesthetized with an intraperitoneal injection of ketamine (80 mg/kg; Ketalar, Pfizer, Zürich, Switzerland) and medetomidine (1 mg/kg; Domitor; Orion Pharma, Espoo, Finland). Pupils were dilated with eye drops (2.5% phenylephrine + 0.5% tropicamide; MIX-Augentropfen, ISPI, Bern, Switzerland), and the anesthetized mice were placed on a temperature-controlled heating table (Roland Consult, Brandenburg, Germany). ERGs were recorded simultaneously from both eyes with gold wire electrodes, which touched the central cornea of each eye and were wetted with 1% methylcellulose (OmniVision, Santa Clara, CA). A gold wire electrode (0.2 mm diameter) placed in the mouth was used as a reference electrode, and another electrode positioned on the tail served as the ground electrode. Strobe flashes of light were presented in a Q400 Ganzfeld bowl, and responses were amplified, averaged, and stored using a RetiScan-RetiPort electrophysiology unit (Roland Consult, Brandenburg, Germany). ERGs were obtained to 0.47 log cd·s/m^2 strobe flash stimuli presented in the dark or superimposed upon a steady adapting field (25 cd/m^2), following a 10 min light adaption period.

Table 1. Primers

Primer name	Primer sequence (5′ – 3′)
tg21inv1	CCAGGGCAGGATCTGAATTC
tg21inv2	CCCTCCATCTAGCCTCAACC
Chr8–01	CCCACCATGTGACAAAACTA
Chr8–03	CAGCTCTGGTAAAGGAGGAA
hPDGF fwd	CCATCTCCAGGTTGAGGC
hPDGF rev	GTCTCTGAGAGCCGAGC
Gpr179 fwd	TGTGCCTGGGTATCTGTTGA
Gpr179 rev	GCTTACACACTTACACACAGATAGAT
Gpr179 insert	GCATGTGCCAAGGGTATCTT

Histology and immunohistochemistry: Mouse eyecups were freshly prepared by removing the cornea and the lens. Following fixation in 4% paraformaldehyde (PFA), the tissue was snap frozen in optimum cutting temperature (OCT) compound or embedded in paraffin, and either 7 µm (OCT) or 5 µm (paraffin) thick sections were cut.

Sagittal paraffin sections at the level of the optic nerve head were stained with hematoxylin and eosin and used for retinal thickness measurements. The thickness of each cellular and plexiform layer was calculated using ImagePro software (Media Cybernetics, Rockville, MD) at six different locations (400, 1,000, and 1,600 µm inferior and superior to the edge of the ONH).

Paraffin sections were rehydrated and, following antigen retrieval, permeabilized and incubated with blocking solution (10% normal goat serum and 1% bovine serum albumin dissolved in TBS (Tris-buffered Saline; 50 mM Tris-HCl, 150 mM NaCl, pH 7.5) supplemented with 0.025% Tween-20) for 1 h. Sections were then incubated with the primary antibody (anti-protein kinase C alpha, 1:500; Sigma Aldrich, Buchs, Switzerland) at 4 °C overnight. As a secondary antibody, a goat anti-mouse Alexa Fluor 488 antibody (1:500; Invitrogen, Carlsbad, CA) was used.

Cryosections were blocked (5% horse serum/0.5% Tween-20 in TBS) for 1 h and incubated with primary antibody (sheep anti-Gpr179 [7] 1:1,000 in 5% horse serum/0.5% Tween-20 in TBS) at 4 °C overnight. A secondary antibody, donkey anti-sheep Alexa Fluor 594 (Invitrogen), was applied in a 1:500 dilution for 45 min. After staining, the sections were mounted using 4',6-diamidino-2-phenylindole dihydrochloride Vectashield (Vector Laboratories, Orton Southgate, UK).

The retinal vasculature was visualized using a published procedure [16]. Briefly, eyes were enucleated and fixed in 2% PFA for 5 min. Following removal of lens and cornea, the sensory retina was dissected out, flattened and postfixed in 4% PFA for another 10 min. Flat mounts were then incubated for 1 h in blocking solution consisting of 1% fetal bovine serum diluted in 0.1% Triton X-100 in phosphate buffered saline. Retinas were incubated overnight in *Griffonia simplicifolia* isolectin IB_4-Alexa488 (Life Technologies, Carlsbad CA) diluted 1:1000 in blocking solution. Following washing steps, flat mounts were mounted using fluorescent mounting medium (DAKO, Baar, Switzerland) and digital images were recorded using a confocal microscope (Zeiss LSM 710; Carl Zeiss, Jena, Germany).

Quantitative reverse transcription polymerase chain reaction for bipolar cell genes: TaqMan Gene expression assays were used to compare expression levels of DBC genes. Following RNA isolation of retinal tissues, reverse transcription was performed using the SuperScript II First-Strand Synthesis System (Invitrogen). PCR amplifications on cDNA were conducted using the TaqMan gene expression assays on a Real-Time PCR System (7900HT; Applied Biosystems, Life Technologies, Foster City, CA) according to the manufacturer's instructions. Values were normalized to control measures, and actin served as the internal standard.

Detection of the Gpr179^{nob5} mutation: To confirm the presence of a mutation in intron 1 of *Gpr179*, mouse-specific primers (*Gpr179* forward, *Gpr179* reverse; Table 1) were designed to amplify an intron fragment that encompassed the transposon insertion site in *Gpr179* mice. Sequencing of a PCR fragment enabled the design of a primer (*Gpr179* insert; Table 1) on the insertion site. To identify the position of the insertion site in the mouse genome, the BLAT program (UCSC Genome Browser) was used.

PCR amplifications were performed as described using an annealing step at 60 °C and a mix of all three *Gpr179* primers (Table 1) and genomic DNA as the template. PCR products were analyzed on 2.5% agarose gels stained with ethidium bromide and visualized using the Versa Doc Imaging System (BioRad).

RESULTS

Identification of a no-b-wave electroretinogram phenotype: During the course of the baseline ERG studies of tg21 animals, we observed that animals from this line lacked the b-wave. In Figure 1, representative ERGs obtained from a tg21 mouse and a C57BL/6 mouse are compared in response to 0.47 log cd s/m^2 stimuli presented under either dark-adapted (left) or light-adapted (right) conditions. Under both adaptation conditions, the ERGs obtained from the tg21 mice were markedly abnormal. In the dark-adapted state, the ERGs of the tg21 mice lacked the b-wave that normally follows the a-wave. Under light-adapted conditions (right), the major positive component of the cone ERG was reduced in the tg21 mice.

Retinal histology, bipolar cell morphology, and retinal vasculature are normal in tg21 no-b-wave mice: To dissect the basis for the nob ERGs of the tg21 mice, we examined the overall retinal structure. In Figure 2A, the retinal cross sections obtained from a non-transgenic mouse with a normal b-wave (left) are compared with those of a tg21 nob mouse (right). All cellular and plexiform layers are present in the tg21 nob retina, which is generally comparable to that of the wild-type (WT) retina. This impression was confirmed when each cellular and plexiform layer was measured. As shown

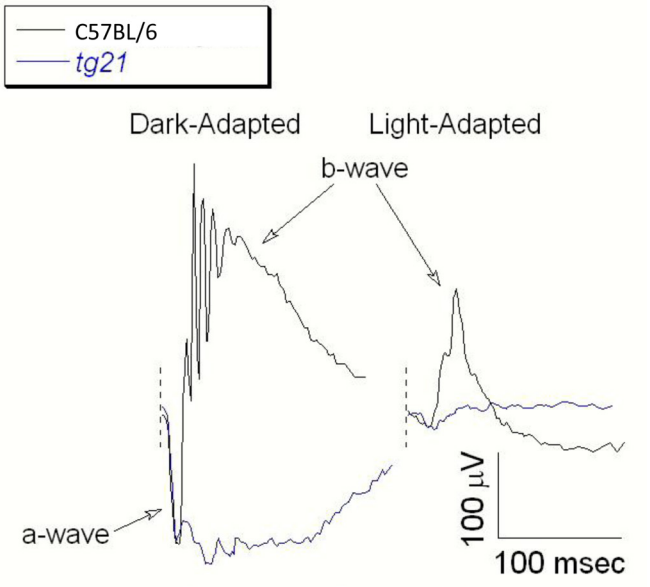

Figure 1. Electroretinograms (ERGs) were recorded from 6-week old tg21 animals (blue tracings) and C57BL/6 WT mice (black tracings) in response to 0.47 log cd·s/m^2 strobe flashes presented under dark-adapted (left) or light-adapted (right) recording conditions. In comparison to the wild type (WT) response, the b-wave component is markedly reduced in tg21 mice.

in Figure 2B, there was no significant difference between the retinal morphology of the WT and tg21 nob mice, including the inner nuclear layer (INL), where DBC cell bodies are located.

To examine whether the ERG phenotype of tg21 nob mice might reflect a loss of DBCs [17], we assessed DBC morphology using the DBC marker anti-protein kinase C alpha. As shown in Figure 3, DBCs are present in the tg21 nob retina, and their appearance is comparable to that of WT DBCs.

ERG b-wave amplitudes are sensitive to changes in ocular blood flow [18] and can be strongly reduced or increased upon changes in inner retinal blood flow [19]. High increases in retinal and blood plasma Epo levels have been associated with changes in the retinal vasculature of mice [19]. To evaluate the vasculature of tg21 nob mice, we used immunohistochemistry on retinal flat mounts to assess retinal blood vessels. No significant difference was detectable in vessel structure (primary, intermediate, and deep plexus) between the tg21 nob and WT animals with a normal ERG b-wave (Figure 4).

The electroretinogram phenotype of tg21 no-b-wave mice is not due to the erythropoietin insertion: The results presented in Figure 2, Figure 3, and Figure 4 indicate that the nob ERG phenotype of tg21 mice is not caused by mechanisms that have been reported in other mouse lines, including abnormal retinal architecture [20], loss of DBCs [17], or alterations in blood flow to the inner retina [19]. To evaluate the possibility that the phenotype reflects a mutation due to the transgene insertion site [21], we used a PCR approach to clone a junction fragment with the 5′ end of the tg21 transgene. Sequence analyses identified a 115 bp fragment from mouse chromosome 8 (chr8:51,016,110–51,016,224, mm10). Examination of the genome in this region indicated that the insertion site was located in a gene desert devoid of any annotated genes. As a consequence, the nob ERG phenotype does not reflect an insertion of the transgene into a gene locus known to be required for normal DBC function.

To determine whether the nob ERG phenotype cosegregated with tg21, we used a standard mapping approach in which tg21 homozygous mice were crossed to DBA/2N mice and the resulting F1 animals were intercrossed (Figure 5A). All F1 mice displayed a normal ERG, indicating that the nob ERG trait is recessive. A total of 98 F2 mice were examined with ERG and genotyped for the presence of a chr8:tg21 junction fragment or the WT allele at the tg21 insertion location (Figure 5B). As summarized in Figure 5A, 19 F2 animals (19.3%) lacked the ERG b-wave, and four of them did not inherit the tg21 transgene. Figure 5B shows the genotyping data for eight mice, including one (mouse #3) that was non-transgenic and had a nob ERG. These results indicate that the nob ERG phenotype and tg21 are inherited independently.

The tg21 background carries the Gpr179^{nob5} mutation: To investigate whether the nob ERG phenotype is due to a mutation in a gene known to be critical to DBC function, we examined the expression levels of *Nyx*, *Gpr179, Grm6*, and *Trpm1* using qRT PCR (TaqMan assays). Figure 6 shows the expression level for these genes in C57BL/6, C3H, *Gpr179*^{nob5}, and tg21 nob mice. We detected only marginal *Gpr179* expression in tg21 nob mice, as well as in the *Gpr179*^{nob5} mutant mice run as a positive control. In the tg21 nob mice, *Gpr179* expression was decreased about 370-fold compared to the C57BL/6 controls (Figure 6), a reduction comparable to that reported in the *Gpr179*^{nob5} mutant mouse [7]. To confirm that GPR179 is reduced, we compared the distribution of GPR179 in the retina of WT and tg21 nob mice. As shown in Figure 7, a robust punctate GPR179 label was observed in the outer plexiform layer of the WT animals with a normal ERG b-wave. In comparison, we did not detect GPR179 in tg21 nob mice. This finding confirmed that the mutation underlying the nob ERG phenotype results in a massive loss of GPR179 expression.

The *Gpr179*^{nob5} mutation arose on a C3H-derived line [7]. To determine whether the mutation underlying the tg21 nob phenotype might be the same mutation, we used

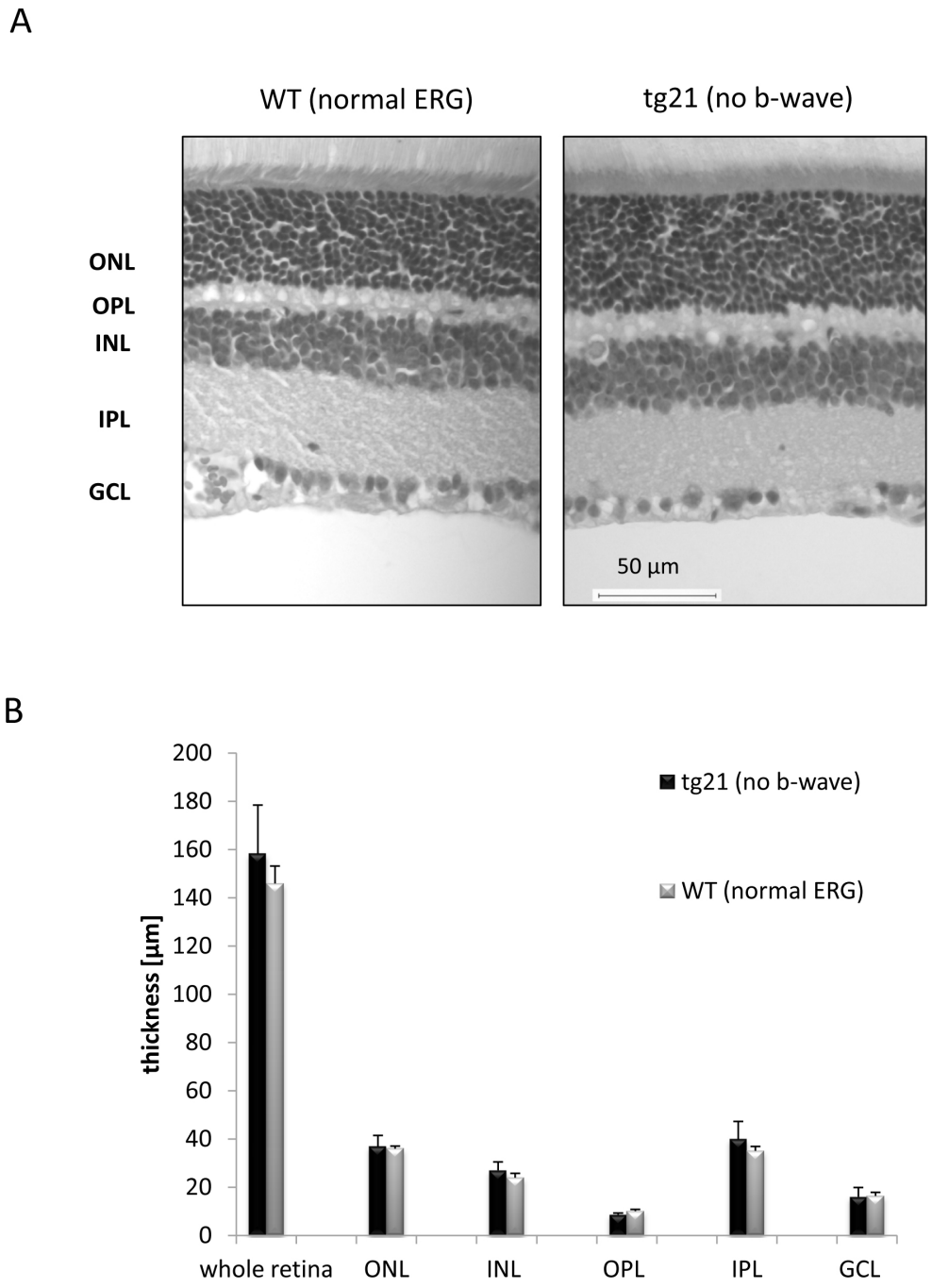

Figure 2. Normal retinal structure is visible in tg21 nob mice. **A**: Retinal cross-sections obtained from 6-week old non-transgenic (left) and tg21 nob (right) littermates. The appearance of the WT and tg21 nob retinas is comparable. **B**: Thickness of individual plexiform or cellular layers was assessed in WT and tg21 nob retinas. There was no significant difference observable in any retinal layer. Bars indicate mean (± S.D. of 4 mice). Abbreviations: ONL represents the outer nuclear layer; OPL represents the outer plexiform layer; INL represents the inner nuclear layer; IPL represents the inner plexiform layer; GCL represents the ganglion cell layer.

primers developed to genotype the *Gpr179*^{nob5} allele (Figure 8). These primers correctly identified each nob ERG mouse we examined (Figure 9), indicating that the *Gpr179*^{nob5} allele underlies the nob ERG phenotype we encountered in the tg21 transgenic line. To confirm that this mutation is identical, we compared the junction fragment sequence of the insertional mutation and found these were identical (data not shown).

Gpr179^{nob5} *allele is present in C3H "sighted" mice*: These data suggest that the *Gpr179*^{nob5} allele arose on a common background, and may be present in other lines derived from C3H. Hoelter and colleagues [13] reported a line of "sighted" C3H.Pde6b^{+} mice in which the *Pde6*^{rd1} locus was replaced by the WT allele, and did not develop the photoreceptor degeneration characteristic of C3H/HeH mice. These mice retained a normal ERG a-wave, but lacked the b-wave [13]. When we examined DNA samples from C3H/HeH and C3H.

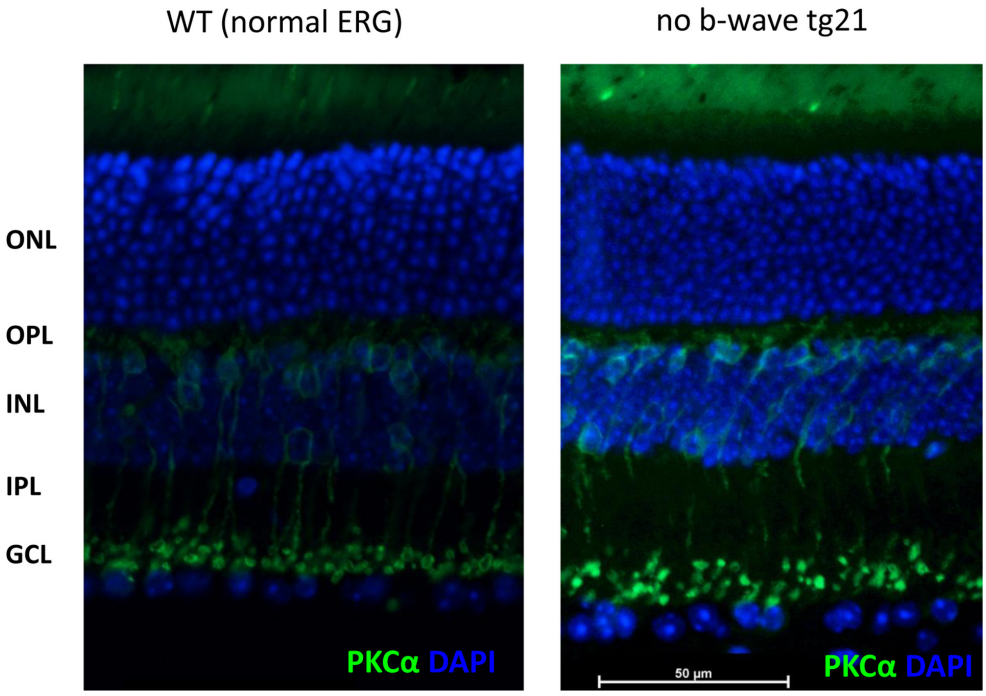

Figure 3. Retinal cross sections were stained for normal depolarizing bipolar cell function using an antibody against protein kinase C alpha (PKCα; green) and with a cell body label (blue). Depolarizing bipolar cells (DBCs) are present in the tg21 no b-wave (nob) retina (right), with a distribution that is comparable to that of non-transgenic (left) littermates.

Pde6b^{+} mice, we observed that C3H.Pde6b^{+} mice carry the *Gpr179*^{nob5} allele (Figure 10).

DISCUSSION

In this study, we evaluated the basis for the nob ERG phenotype identified in a line of transgenic mice overexpressing Epo in the brain and the retina. The nob ERG phenotype does not reflect a loss of DBCs or some other abnormality in the retinal structure, as all measures in the tg21 nob retinas were comparable to WT. When tg21 mice were crossed to a WT strain (DBA/2N), we observed that the nob ERG phenotype was inherited independently of the tg21 transgene. This observation proves that the nob ERG phenotype is not caused by the tg21 transgene product or insertion site. When we examined the expression of several genes required for normal DBC function, we found that the expression of *Gpr179* was markedly reduced. Further analysis indicated that the nob mice studied here carry the *Gpr179*^{nob5} allele recently identified in a mouse line also derived from C3H [7]. To evaluate whether this allele is present elsewhere, we examined another

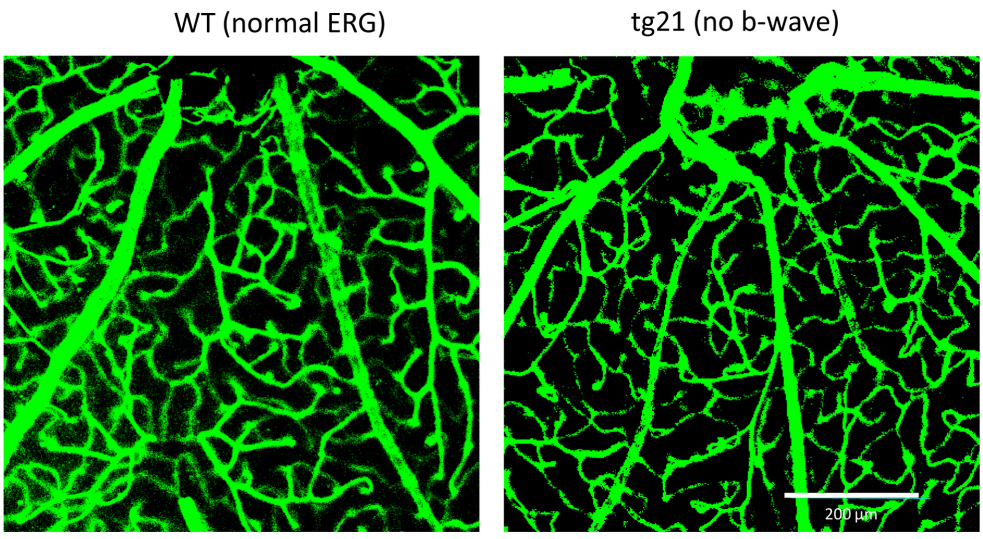

Figure 4. Comparison of retinal vasculature performed using retinal whole mounts of non-transgenic (left) and tg21 (right) littermates. Whole mounts were prepared with the inner retina facing upward, and stained for vascular endothelial cells using isolectin IB4.

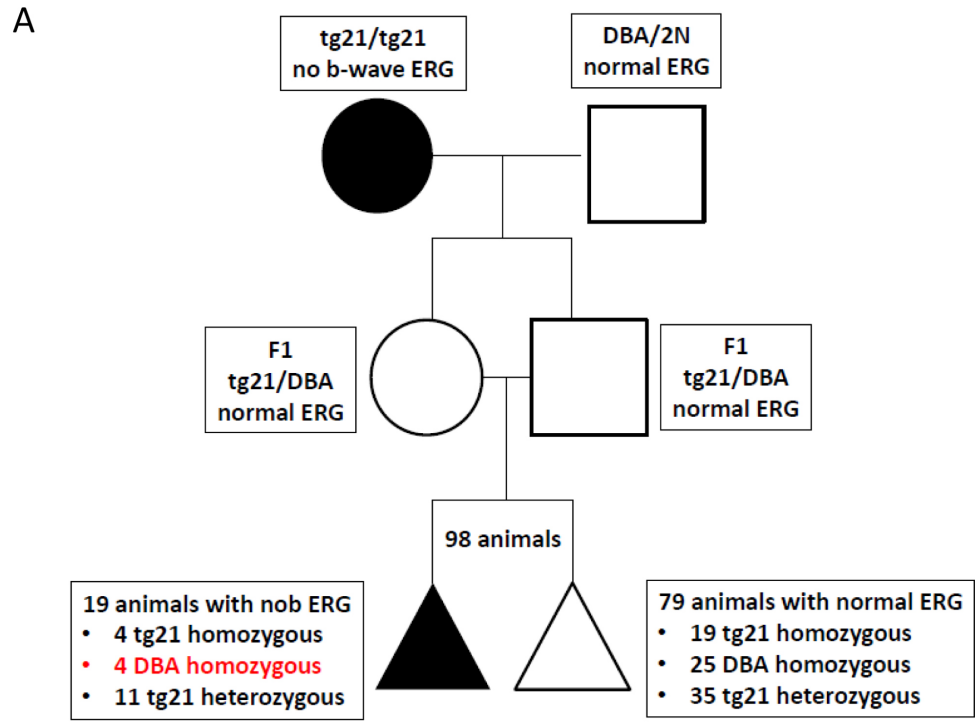

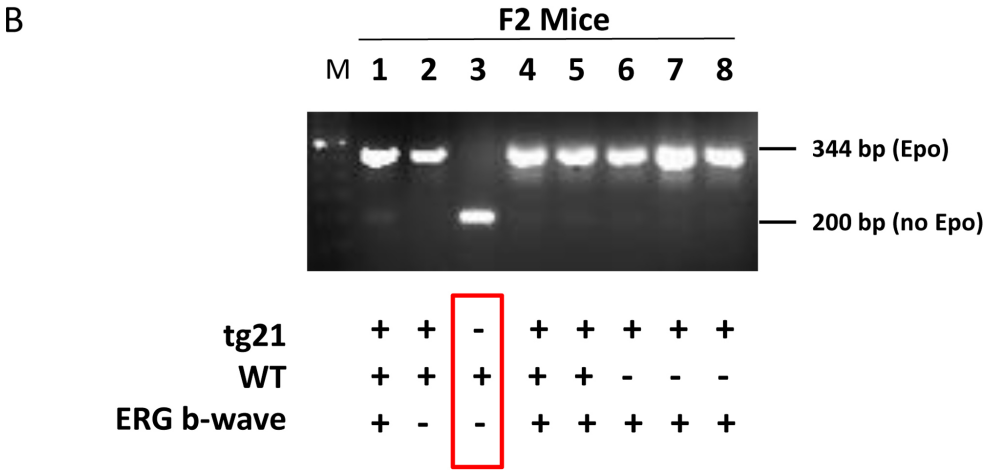

Figure 5. The nob ERG phenotype does not segregate with the tg21 transgene. **A**: Pedigree of a two-generation cross between tg21 no-b-wave and DBA/2N mice. All F1 offspring had normal electroretinograms (ERGs). **A**: Of 98 F2 progeny, 19 mice had a no-b-wave (nob) ERG phenotype; of these, four were non-transgenic (DBA). **B**: Genotyping demonstrated that tg21 and the nob ERG phenotype do not cosegregate. Note that mouse #3 is non-transgenic and has a nob ERG.

nob mouse, the "sighted" C3H.Pde6b^{+} mouse. The *Gpr179*^{nob5} allele was also present in that line in which the *Pde6b*^{rd1} allele was removed. However, the mutation was not found in C3H/HeH mice that carry the *Pde6*^{rd1} allele. These results indicate that the *Gpr179*^{nob5} allele was present in the background strain on which the tg21 transgenic line was established or was carried by the subsequent strains used to maintain this line. In that regards, it is possible that tg21 bred in other research laboratories do not carry the *Gpr179*^{nob5} allele, since the tg21 transgene and the *Gpr179*^{nob5} allele might be inherited independently resulting in the potential for the WT *Gpr179* allele to be crossed into the transgenic line.

Identifying the *Gpr179*^{nob5} allele in a C3H-derived line raises the possibility that it may be present in additional mouse lines. There is certainly precedent for an allele that negatively impacts retinal function to be widespread. For example, the *Pdeb6*^{rd1} allele results in a rapid degeneration of rod and cone photoreceptors and has been identified in many mouse strains [22,23]. The *Crb1*^{rd8} allele causes ocular lesions [24] and has been identified in multiple inbred mouse strains [25]. The *Gnat2*^{cpfl3} results in one photoreceptor dysfunction

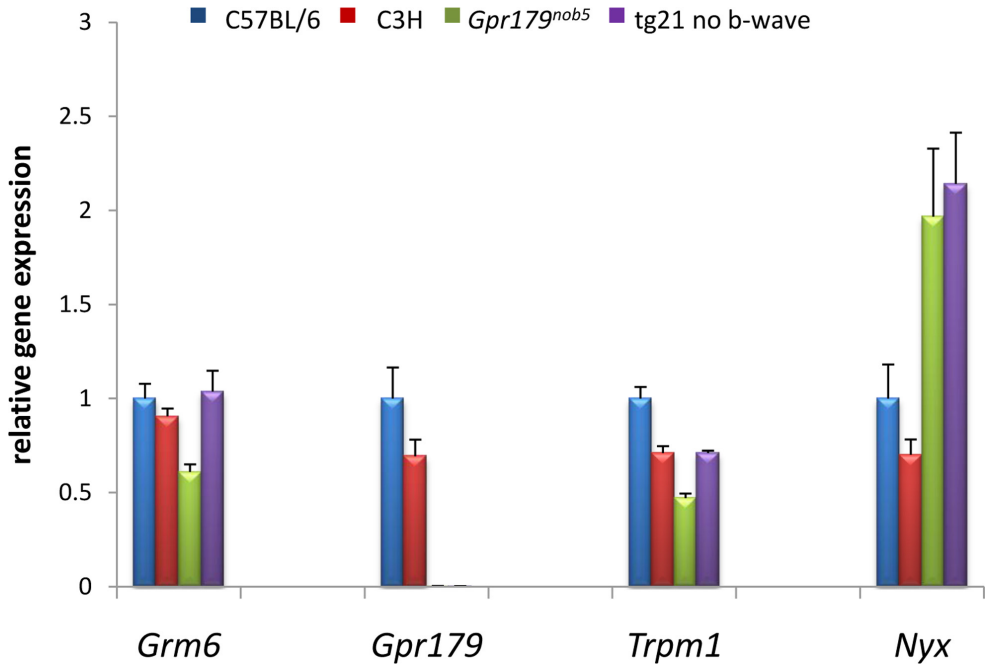

Figure 6. Expression levels of several genes required for normal depolarizing bipolar cell (DBC) function in several mouse lines. Note that expression of *Gpr179* was decreased 370-fold in the tg21 no b-wave (nob) mice and in *Gpr179*^{nob5} mutant mice. Other depolarizing bipolar cell (DBC) genes were expressed at normal or slightly higher than normal levels in the tg21 nob and *Gpr179*^{nob5} mice. Values were normalized to control measures and actin served as the internal standard. Values are expressed as mean±SD (n=3).

and was recently identified in several inbred lines [26]. We have not conducted a thorough survey of inbred mouse lines, but the *Gpr179*^{nob5} allele could be present in additional mouse lines, particularly those related to C3H, as each line known to carry this allele was derived from that background. Although the *Gpr179*^{nob5} allele was not present in any commercially available C3H lines, our observation that the identical mutation has been identified on both sides of the Atlantic on a sighted C3H background suggests this allele may be widespread, although its presence could be masked by the presence of the *rd1* allele. In conclusion, should a nob ERG phenotype be encountered during the course of evaluating

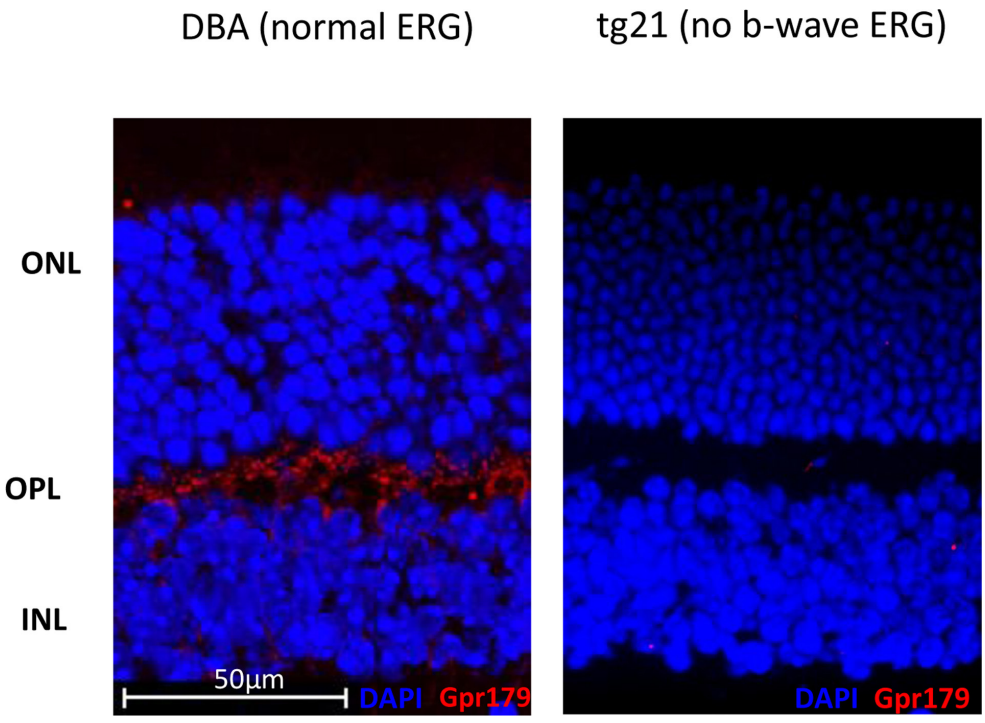

Figure 7. Retinal cross-sections obtained from tg21 mice no b-wave mice and control littermates were stained for GPR179. Positive staining is seen as punctate distribution in the outer plexiform layer of control mice, and is absent from retinas of tg21 no b-wave (nob) mice. Abbreviations: OPL represents the outer plexiform layer; ONL represents the outer nuclear layer; INL represents the inner nuclear layer.

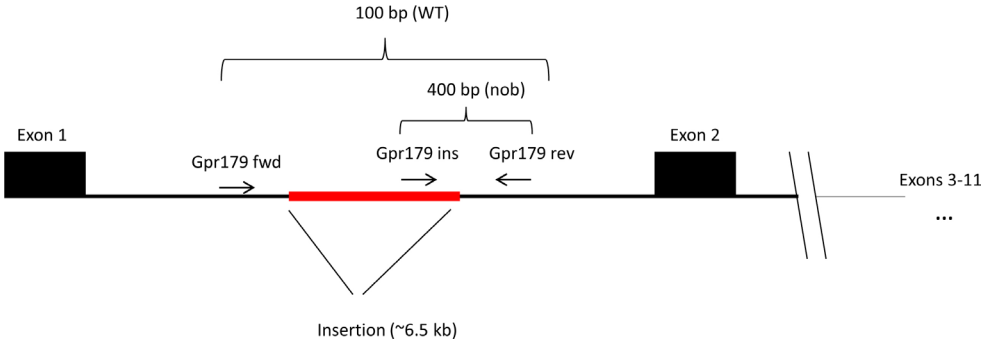

Figure 8. Representation of a 6.5 kb insertion in intron 1 of *Gpr179* identified with polymerase chain reaction using an intron-specific primer and subsequent Sanger sequencing. The schematic indicates the presence of the mutation in intron 1 of *Gpr179*. The sequence obtained with PCR with an intron-specific primer (*Gpr179* rev) was used to design the mutation-specific primer. All three *Gpr179* primers (Table 1) were used for genotyping.

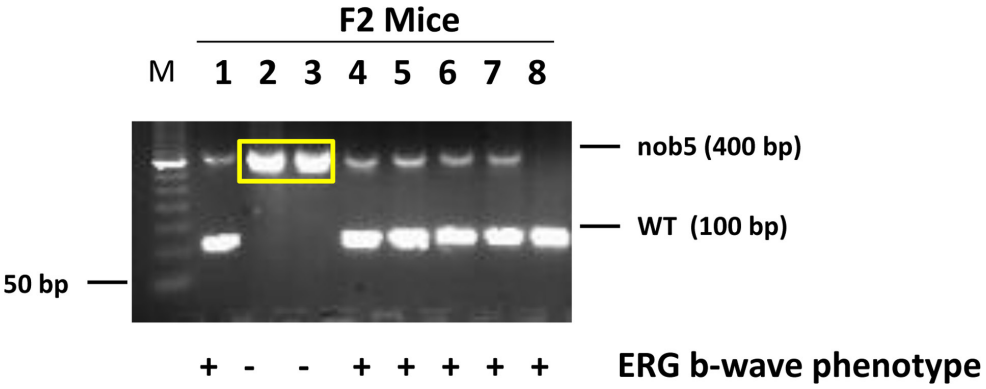

Figure 9. Agarose gel visualization of genotyped genomic deoxyribonucleic acid samples of mice screened for the *Gpr179*^{nob5} allele and examined with electroretinogram. The yellow box highlights the observation that the no-b-wave (nob) electroretinogram (ERG) phenotype was observed only in mice that were homozygous for the *Gpr179*^{nob5} allele.

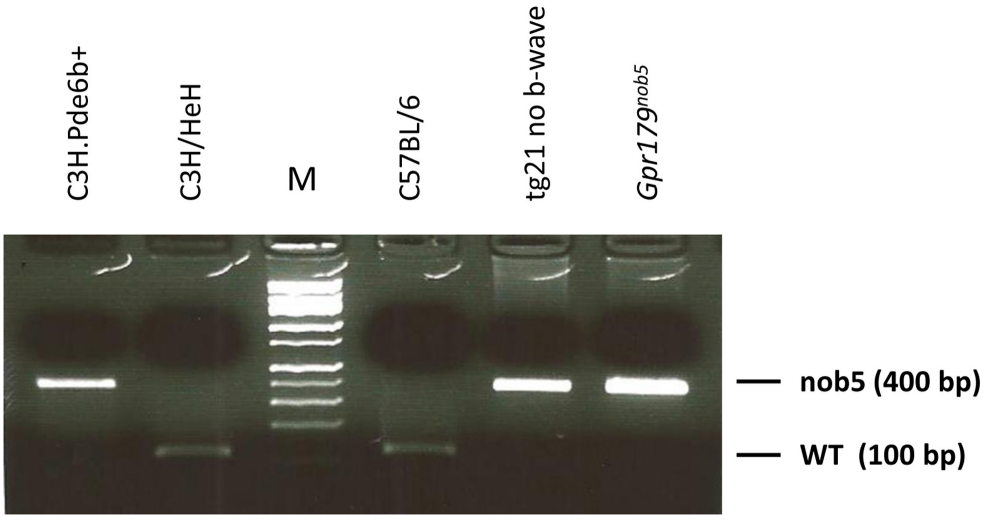

Figure 10. Polymerase chain reaction was performed on genomic deoxyribonucleic acid obtained from two C3H lines (C3H/HeH and C3H.Pde6b^{+}) using the *Gpr179*^{nob5} primers. Control mice were C57BL6 and the well-described *nob5* mouse mutant [7]. C3H.Pde6b^{+} was homozygous mutated for *Gpr179*.

a mouse line, it would be efficient to evaluate whether the *Gpr179*^{nob5} allele may be responsible. If this is the case, the mutation has to be outcrossed before the animals are used for visual function experiments.

ACKNOWLEDGMENTS

The authors thank Dr. Markus Tschopp for his valuable scientific input as well as Agathe Duda and Federica Bisignani for their excellent technical assistance. This work was supported by funding from the National Institutes of Health (R01EY12354 (RGG); R21EY21852 (NSP, RGG)), the Foundation Fighting Blindness, the Department of Veterans Affairs and unrestricted grants from Research to Prevent Blindness to the University of Louisville and the Cleveland Clinic Lerner College of Medicine of Case Western Reserve University and from the Berne University Research Foundation.

REFERENCES

1. Grimm C, Wenzel A, Groszer M, Mayser H, Seeliger M, Samardzija M, Bauer C, Gassmann M, Reme CE. HIF-1-induced erythropoietin in the hypoxic retina protects against light-induced retinal degeneration. Nat Med 2002; 8:718-24. [PMID: 12068288].
2. Grimm C, Wenzel A, Stanescu D, Samardzija M, Hotop S, Groszer M, Naash M, Gassmann M, Reme C. Constitutive overexpression of human erythropoietin protects the mouse retina against induced but not inherited retinal degeneration. J Neurosci 2004; 24:5651-8. [PMID: 15215287].
3. Rex TS, Wong Y, Kodali K, Merry S. Neuroprotection of photoreceptors by direct delivery of erythropoietin to the retina of the retinal degeneration slow mouse. Exp Eye Res 2009; 89:735-40. [PMID: 19591826].
4. Penn RD, Hagins WA. Signal transmission along retinal rods and the origin of the electroretinographic a-wave. Nature 1969; 223:201-4. [PMID: 4307228].
5. Stockton RA, Slaughter MM. B-wave of the electroretinogram. A reflection of ON bipolar cell activity. J Gen Physiol 1989; 93:101-22. [PMID: 2915211].
6. Gregg RG, Mukhopadhyay S, Candille SI, Ball SL, Pardue MT, McCall MA, Peachey NS. Identification of the gene and the mutation responsible for the mouse nob phenotype. Invest Ophthalmol Vis Sci 2003; 44:378-84. [PMID: 12506099].
7. Peachey NS, Ray TA, Florijn R, Rowe LB, Sjoerdsma T, Contreras-Alcantara S, Baba K, Tosini G, Pozdeyev N, Iuvone PM, Bojang P Jr, Pearring JN, Simonsz HJ, van GM, Birch DG, Traboulsi EI, Dorfman A, Lopez I, Ren H, Goldberg AF, Nishina PM, Lachapelle P, McCall MA, Koenekoop RK, Bergen AA, Kamermans M and Gregg RG. GPR179 is required for depolarizing bipolar cell function and is mutated in autosomal-recessive complete congenital stationary night blindness. Am J Hum Genet 2012; 90:331-9. [PMID: 22325362].
8. Maddox DM, Vessey KA, Yarbrough GL, Invergo BM, Cantrell DR, Inayat S, Balannik V, Hicks WL, Hawes NL, Byers S, Smith RS, Hurd R, Howell D, Gregg RG, Chang B, Naggert JK, Troy JB, Pinto LH, Nishina PM, McCall MA. Allelic variance between GRM6 mutants, Grm6nob3 and Grm6nob4 results in differences in retinal ganglion cell visual responses. J Physiol 2008; 586:4409-24. [PMID: 18687716].
9. Koike C, Numata T, Ueda H, Mori Y, Furukawa T. TRPM1: a vertebrate TRP channel responsible for retinal ON bipolar function. Cell Calcium 2010; 48:95-101. [PMID: 20846719].
10. Morgans CW, Zhang J, Jeffrey BG, Nelson SM, Burke NS, Duvoisin RM, Brown RL. TRPM1 is required for the depolarizing light response in retinal ON-bipolar cells. Proc Natl Acad Sci USA 2009; 106:19174-8. [PMID: 19861548].
11. Peachey NS, Pearring JN, Bojang P Jr, Hirschtritt ME, Sturgill-Short G, Ray TA, Furukawa T, Koike C, Goldberg AF, Shen Y, McCall MA, Nawy S, Nishina PM, Gregg RG. Depolarizing bipolar cell dysfunction due to a Trpm1 point mutation. J Neurophysiol 2012; 108:2442-51. [PMID: 22896717].
12. Shen Y, Heimel JA, Kamermans M, Peachey NS, Gregg RG, Nawy S. A transient receptor potential-like channel mediates synaptic transmission in rod bipolar cells. J Neurosci 2009; 29:6088-93. [PMID: 19439586].
13. Hoelter SM, Dalke C, Kallnik M, Becker L, Horsch M, Schrewe A, Favor J, Klopstock T, Beckers J, Ivandic B, Gailus-Durner V, Fuchs H. Hrabe de AM, Graw J and Wurst W. "Sighted C3H" mice–a tool for analysing the influence of vision on mouse behaviour? Front Biosci 2008; 13:5810-23. [PMID: 18508624].
14. Ruschitzka FT, Wenger RH, Stallmach T, Quaschning T. de WC, Wagner K, Labugger R, Kelm M, Noll G, Rulicke T, Shaw S, Lindberg RL, Rodenwaldt B, Lutz H, Bauer C, Luscher TF and Gassmann M. Nitric oxide prevents cardiovascular disease and determines survival in polyglobulic mice overexpressing erythropoietin. Proc Natl Acad Sci USA 2000; 97:11609-13. [PMID: 11027359].
15. Soliz J, Joseph V, Soulage C, Becskei C, Vogel J, Pequignot JM, Ogunshola O, Gassmann M. Erythropoietin regulates hypoxic ventilation in mice by interacting with brainstem and carotid bodies. J Physiol 2005; 568:559-71. [PMID: 16051624].
16. Fruttiger M. Development of the mouse retinal vasculature: angiogenesis versus vasculogenesis. Invest Ophthalmol Vis Sci 2002; 43:522-7. [PMID: 11818400].
17. Peachey NS, Quiambao AB, Xu X, Pardue MT, Roveri L, McCall MA, Al-Ubaidi MR. Loss of bipolar cells resulting from the expression of bcl-2 directed by the IRBP promoter. Exp Eye Res 2003; 77:477-83. [PMID: 12957146].
18. Tazawa Y, Seaman AJ. The electroretinogram of the living extracorporeal bovine eye. The influence of anoxia and hypothermia. Invest Ophthalmol 1972; 11:691-8. [PMID: 5044721].

19. Ye X, Wang Y, Cahill H, Yu M, Badea TC, Smallwood PM, Peachey NS, Nathans J. Norrin, frizzled-4, and Lrp5 signaling in endothelial cells controls a genetic program for retinal vascularization. Cell 2009; 139:285-98. [PMID: 19837032].

20. Chang B, Heckenlively JR, Bayley PR, Brecha NC, Davisson MT, Hawes NL, Hirano AA, Hurd RE, Ikeda A, Johnson BA, McCall MA, Morgans CW, Nusinowitz S, Peachey NS, Rice DS, Vessey KA, Gregg RG. The nob2 mouse, a null mutation in Cacna1f: anatomical and functional abnormalities in the outer retina and their consequences on ganglion cell visual responses. Vis Neurosci 2006; 23:11-24. [PMID: 16597347].

21. Keller SA, Jones JM, Boyle A, Barrow LL, Killen PD, Green DG, Kapousta NV, Hitchcock PF, Swank RT, Meisler MH. Kidney and retinal defects (Krd), a transgene-induced mutation with a deletion of mouse chromosome 19 that includes the Pax2 locus. Genomics 1994; 23:309-20. [PMID: 7835879].

22. Chang B, Hurd R, Wang J, Nishina P. Survey of common eye diseases in laboratory mouse strains. Invest Ophthalmol Vis Sci 2013; 54:4974-81. [PMID: 23800770].

23. Pittler SJ, Keeler CE, Sidman RL, Baehr W. PCR analysis of DNA from 70-year-old sections of rodless retina demonstrates identity with the mouse rd defect. Proc Natl Acad Sci USA 1993; 90:9616-9. [PMID: 8415750].

24. Mehalow AK, Kameya S, Smith RS, Hawes NL, Denegre JM, Young JA, Bechtold L, Haider NB, Tepass U, Heckenlively JR, Chang B, Naggert JK, Nishina PM. CRB1 is essential for external limiting membrane integrity and photoreceptor morphogenesis in the mammalian retina. Hum Mol Genet 2003; 12:2179-89. [PMID: 12915475].

25. Mattapallil MJ, Wawrousek EF, Chan CC, Zhao H, Roychoudhury J, Ferguson TA, Caspi RR. The Rd8 mutation of the Crb1 gene is present in vendor lines of C57BL/6N mice and embryonic stem cells, and confounds ocular induced mutant phenotypes. Invest Ophthalmol Vis Sci 2012; 53:2921-7. [PMID: 22447858].

26. Chang B, Dacey MS, Hawes NL, Hitchcock PF, Milam AH. tmaca-Sonmez P, Nusinowitz S and Heckenlively JR. Cone photoreceptor function loss-3, a novel mouse model of achromatopsia due to a mutation in Gnat2. Invest Ophthalmol Vis Sci 2006; 47:5017-21. [PMID: 17065522].

Articles are provided courtesy of Emory University and the Zhongshan Ophthalmic Center, Sun Yat-sen University, P.R. China. The print version of this article was created on 31 December 2013. This reflects all typographical corrections and errata to the article through that date. Details of any changes may be found in the online version of the article.